Inelastic Neutron Scattering

theoretical background

Why Neutron is suitable for molecular dynamics?

$$E = \frac{1}{2} m v^2$$

$$\lambda = \frac{h}{mv}$$

$$E = \frac{h^2}{2m\lambda^2}$$

$$\lambda : 0.5 \sim 10 \,\text{Å}$$

$$E : 300 \sim 0.8 meV$$

$$note : kT \sim 20 meV$$

$$E = 5.228 \times 10^{-6} v^2 = 81.79 \lambda^2$$

$$\vec{p} = \hbar\vec{k}$$

$$E = \frac{p^2}{2m} = \frac{\hbar^2 k^2}{2m}$$

$$\vec{q} = \hbar\vec{k}_1 - \hbar\vec{k}_0$$

$$\Delta E = \hbar w_1 - \hbar w_0 = \frac{\hbar^2 k_1^2}{2m} - \frac{\hbar^2 k_0^2}{2m}$$

$$q^2 = k_1^2 + k_0^2 - 2k_1 k_0 \cos 2\theta$$

$\Delta E = 0$, elastic scattering

$\Delta E \neq 0$, *in*elastic scattering

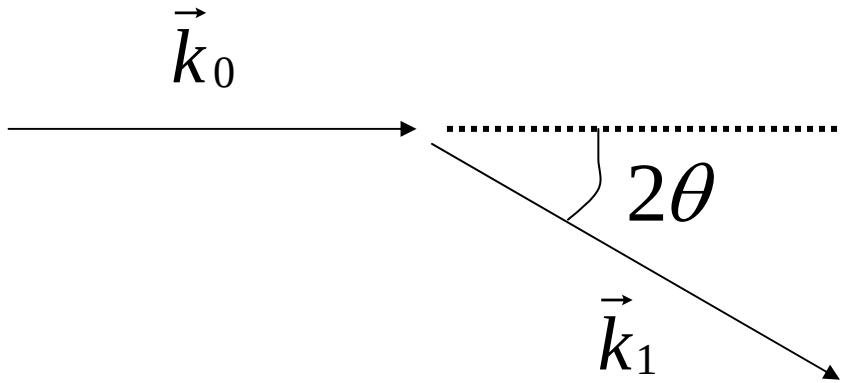

$$A(\vec{q}) = \int \rho(\vec{r}) e^{-i\vec{r}\cdot\vec{q}} d\vec{r}$$

SLDD

$$\rho(\vec{r}) = \rho_u(\vec{r}) * z(\vec{r})$$

FT

IFT

Scattering amplitude

$$A(\vec{q}) = F(\vec{q})Z(\vec{q})$$

Form factor

lattice factor

autocorrelation

$$\Gamma_\rho(\vec{r})$$
$$= V\left\langle \rho(\vec{u})\rho(\vec{u}')\right\rangle$$
$$= \int \rho(\vec{r})\rho(\vec{u}+\vec{r})d\vec{u}$$

X

squaring

$$I(\vec{q})$$
$$= A(\vec{q})\cdot A^*(\vec{q})$$

$\Gamma_\rho(\vec{r})$

FT

IFT

$I(\vec{q})$

Autocorrelation ftn

$$I(\vec{q}) = \int \Gamma_\rho(\vec{r}) e^{-i\vec{r}\cdot\vec{q}} d\vec{r}$$

structure analysis, $k_1 = k_0$

no E change

$$\frac{d\sigma}{d\Omega} = \left\langle \left| \sum_j b_j e^{-i\vec{r}_j \cdot \vec{q}} \right|^2 \right\rangle = \sum_j \sum_k b_j b_k \left\langle e^{-i\vec{r}_j \cdot \vec{q}} e^{i\vec{r}_k \cdot \vec{q}} \right\rangle$$

differential scattering cross-section in the static approximation

van Hove correlation ftn

intermediate scattering factor

dynamic structure factor

$$G(r,t) \longleftrightarrow F(\vec{q},t) \longleftrightarrow S(q,w)$$

FT in space

FT in time

Inelastic scattering cross-section

double differential scattering cross-section

$$\frac{d^2\sigma}{d\Omega dw} = \frac{k_1}{k_0}\frac{1}{2\pi}\sum_j\sum_k b_j b_k \int_{-\infty}^{\infty} \left\langle e^{-i\vec{r}_j(t)\cdot\vec{q}} e^{i\vec{r}_k(0)\cdot\vec{q}} \right\rangle e^{iwt} dt$$

flux of neutrons at the detector
dep. on the velocity of neutron

double differential scattering cross-section

$$\frac{d^2\sigma}{d\Omega dw} = \frac{k_1}{k_0}\frac{1}{2\pi}\sum_j\sum_k b_j b_k \int_{-\infty}^{\infty} \left\langle e^{-i\vec{r}_j(t)\cdot\vec{q}} e^{i\vec{r}_k(0)\cdot\vec{q}} \right\rangle e^{iwt} dt$$

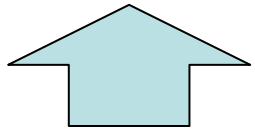

$$\frac{d\sigma}{d\Omega} = \left\langle \left| \sum_j b_j e^{-i\vec{r}_j\cdot\vec{q}} \right|^2 \right\rangle = \sum_j\sum_k b_j b_k \left\langle e^{-i\vec{r}_j\cdot\vec{q}} e^{i\vec{r}_k\cdot\vec{q}} \right\rangle$$

differential scattering cross-section in the static approximation

intermediate scattering function

$$F(q,t) = \frac{1}{N} \sum_j \sum_k \left\langle e^{-i\vec{r}_j(t)\cdot\vec{q}} e^{i\vec{r}_k(0)\cdot\vec{q}} \right\rangle$$

$$\Rightarrow \quad \frac{d^2\sigma}{d\Omega dw} = \frac{k_1}{k_0} b^2 N \int_{-\infty}^{\infty} F(q,t) e^{iwt} dt$$

time-dep pair distribution function (van Hove correlation ftn)

$$G(r,t) = \frac{1}{(2\pi)^3} \int_{-\infty}^{\infty} F(q,t) e^{i\vec{q}\cdot\vec{r}} dq$$

$$\Rightarrow \quad \frac{d^2\sigma}{d\Omega dw} = \frac{k_1}{k_0} b^2 N \frac{1}{2\pi} \int_{-\infty}^{\infty} \int_V G(r,t) e^{-i\left(\vec{q}\cdot\vec{r} - wt\right)} dt$$

Dynamic structure factor

$$S(q,w)$$

$$= \frac{k_1}{k_0} b^2 N \frac{1}{2\pi} \int_{-\infty}^{\infty} F(\vec{q},t) e^{iwt} dt$$

$$= \frac{k_1}{k_0} b^2 N \frac{1}{2\pi} \int_{-\infty}^{\infty} \int_V G(r,t) e^{-i\left(\vec{q}\cdot\vec{r}-wt\right)} d\vec{r} dt$$

$$\frac{d^2\sigma}{d\Omega dw} = \frac{k_1}{k_0} b^2 N \; S(\vec{q},w)$$

van Hove correlation ftn

intermediate scattering factor

dynamic structure factor

$$G(r,t) \longleftrightarrow F(\vec{q},t) \longleftrightarrow S(q,w)$$

FT in space

FT in time

$$G(r,t) = \frac{1}{N}\sum_{j}^{N}\sum_{k}^{N}\frac{1}{(2\pi)^3}\int_{-\infty}^{\infty}\left\langle e^{-i\vec{r}_j(t)\cdot\vec{q}}e^{i\vec{r}_k(0)\cdot\vec{q}}\right\rangle e^{i\vec{r}\cdot\vec{q}}d\vec{q}$$

$$\delta(w) = \frac{1}{2\pi}\int_{-\infty}^{\infty}e^{iwt}dt$$

$$\delta(r-a) = \frac{1}{(2\pi)^3}\int_{-\infty}^{\infty}e^{-i\vec{q}\cdot\vec{a}}e^{i\vec{q}\cdot\vec{r}}d\vec{q}$$

$$G(r,t) = \frac{1}{N}\sum_{j}^{N}\sum_{k}^{N}\left\langle \delta\left[\vec{r} - \left\{\vec{r}_j(t) - \vec{r}_k(0)\right\}\right]\right\rangle$$

$$G(r,t) = \sum_{j}^{N}\sum_{k}^{N}\left\langle \delta\left[\vec{r} - \left\{\vec{r}_j(t) - \vec{r}_1(0)\right\}\right]\right\rangle$$

For instance, when t~0

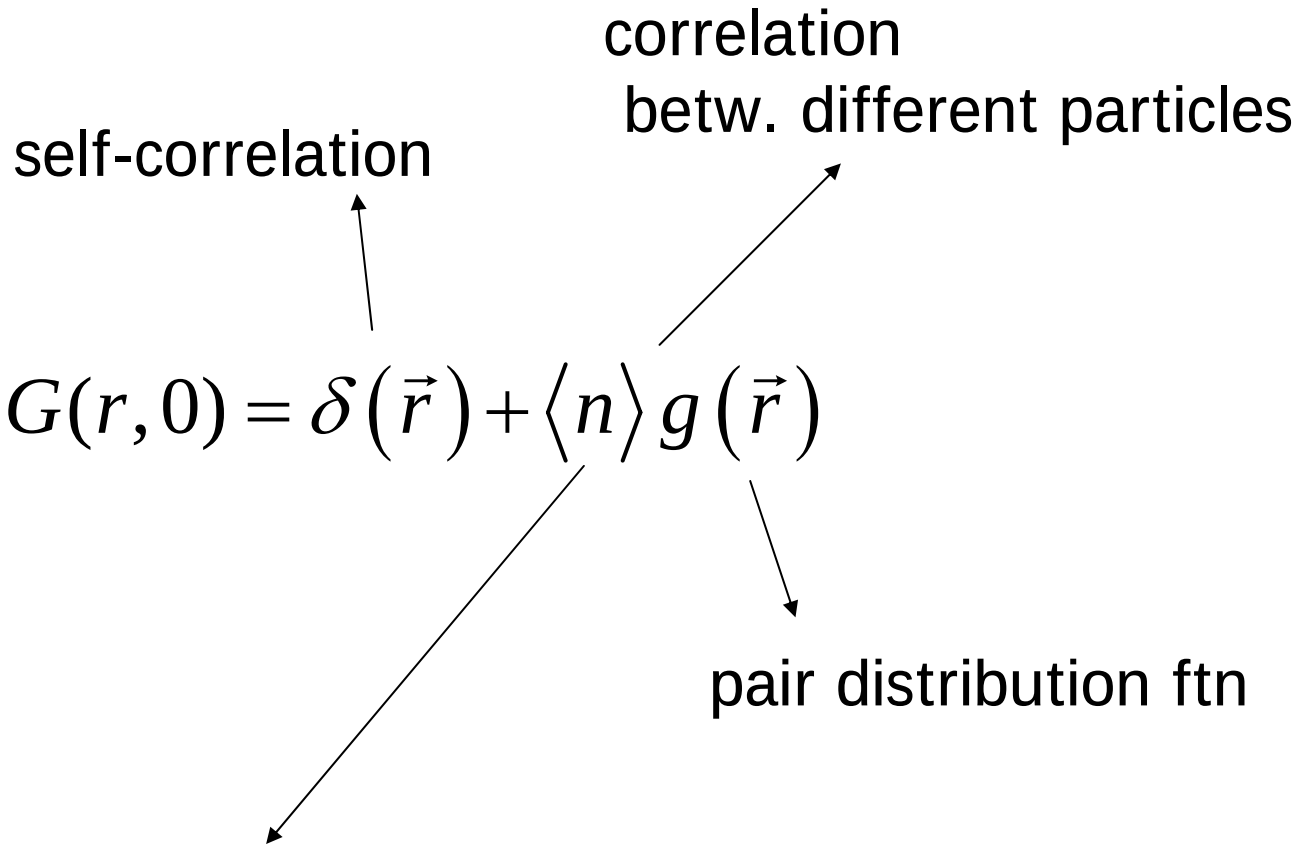

at t=0

$$G(r,0) = \delta(\vec{r}) + \langle n \rangle g(\vec{r})$$

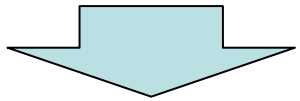

at a certain t

$$G(\vec{r},t) = G_S(\vec{r},t) + G_d(\vec{r},t)$$

correlation betw. different particles

probability that
after seeing a particle at the origin at time 0
we see a different particle at r at t

$$\lim_{r\to\infty} G_d(\vec{r},t) = \lim_{t\to\infty} G_d(\vec{r},t) \sim \langle n \rangle$$

self-correlation

motion of a single particle

$$\lim_{r\to\infty} G_S(\vec{r},t) = \lim_{t\to\infty} G_S(\vec{r},t) = 1/V \sim 0$$

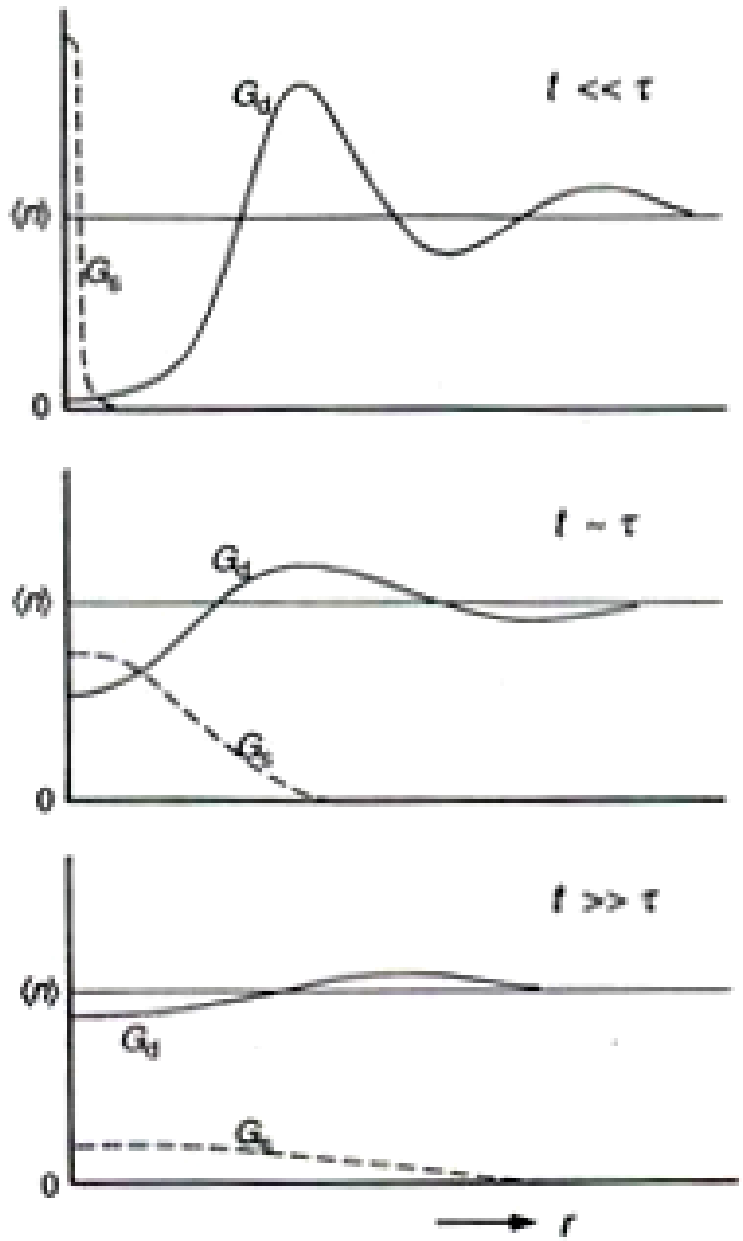

Figure 8.3 Qualitative behavior of the van Hove correlation functions. The full curve is $G_d(r, t)$ and the broken curve is $G_s(r, t)$. (After van Hove.[3])

Coherent and incoherent scattering

$$\frac{d^2\sigma}{d\Omega dw} = \frac{k_1}{k_0}\frac{1}{2\pi}\sum_j\sum_k \left\langle b_j b_k \right\rangle \int_{-\infty}^{\infty} \left\langle e^{-i\vec{r}_j(t)\cdot\vec{q}} e^{i\vec{r}_k(0)\cdot\vec{q}} \right\rangle e^{iwt} dt$$

$$b_{coh} = \left\langle b \right\rangle$$

$$b_{inc} = \left(\left\langle b^2 \right\rangle - \left\langle b \right\rangle^2 \right)^{1/2}$$

$$\frac{d^2\sigma}{d\Omega dw} = \frac{k_1}{k_0}\frac{\left\langle b^2 \right\rangle}{2\pi}\sum_j \int_{-\infty}^{\infty} \left\langle e^{-i\vec{r}_j(t)\cdot\vec{q}} e^{i\vec{r}_k(0)\cdot\vec{q}} \right\rangle e^{iwt} dt$$

$$+\frac{k_1}{k_0}\frac{\left\langle b \right\rangle^2}{2\pi}\sum_{j\neq k}\sum \int_{-\infty}^{\infty} \left\langle e^{-i\vec{r}_j(t)\cdot\vec{q}} e^{i\vec{r}_k(0)\cdot\vec{q}} \right\rangle e^{iwt} dt$$

$$\frac{d^2\sigma}{d\Omega dw} = \frac{k_1}{k_0}\frac{b_{inc}^2}{2\pi}\sum_j \int_{-\infty}^{\infty} \left\langle e^{-i\vec{r}_j(t)\cdot\vec{q}} e^{i\vec{r}_k(0)\cdot\vec{q}} \right\rangle e^{iwt} dt$$

$$+\frac{k_1}{k_0}\frac{b_{coh}^2}{2\pi}\sum_j\sum_k \int_{-\infty}^{\infty} \left\langle e^{-i\vec{r}_j(t)\cdot\vec{q}} e^{i\vec{r}_k(0)\cdot\vec{q}} \right\rangle e^{iwt} dt$$

$$\left(\frac{d^2\sigma}{d\Omega dw}\right)_{inc} = \frac{k_1}{k_0}\frac{Nb_{inc}^2}{2\pi}\int_{-\infty}^{\infty}\int Gs(r,t)e^{-i(\vec{r}\cdot\vec{q}-wt)}d\vec{r}dt$$

$$\left(\frac{d^2\sigma}{d\Omega dw}\right)_{coh} = \frac{k_1}{k_0}\frac{Nb_{coh}^2}{2\pi}\int_{-\infty}^{\infty}\int Gs(r,t)e^{-i(\vec{r}\cdot\vec{q}-wt)}d\vec{r}dt$$

$$F(\vec{q},t) = F_S(\vec{q},t) + F_d(\vec{q},t)$$

$$S(\vec{q},w) = S_S(\vec{q},w) + S_d(\vec{q},w)$$

$$\left(\frac{d^2\sigma}{d\Omega dw}\right)_{inc} = \frac{k_1}{k_0}b_{inc}^2 NS_s(\vec{q},w)$$

$$F(q,t) = \frac{1}{N}\sum_j^N \left\langle e^{-i\left(\vec{r}_j(t)-\vec{r}_j(0)\right)\cdot\vec{q}} \right\rangle$$

simple models of motion

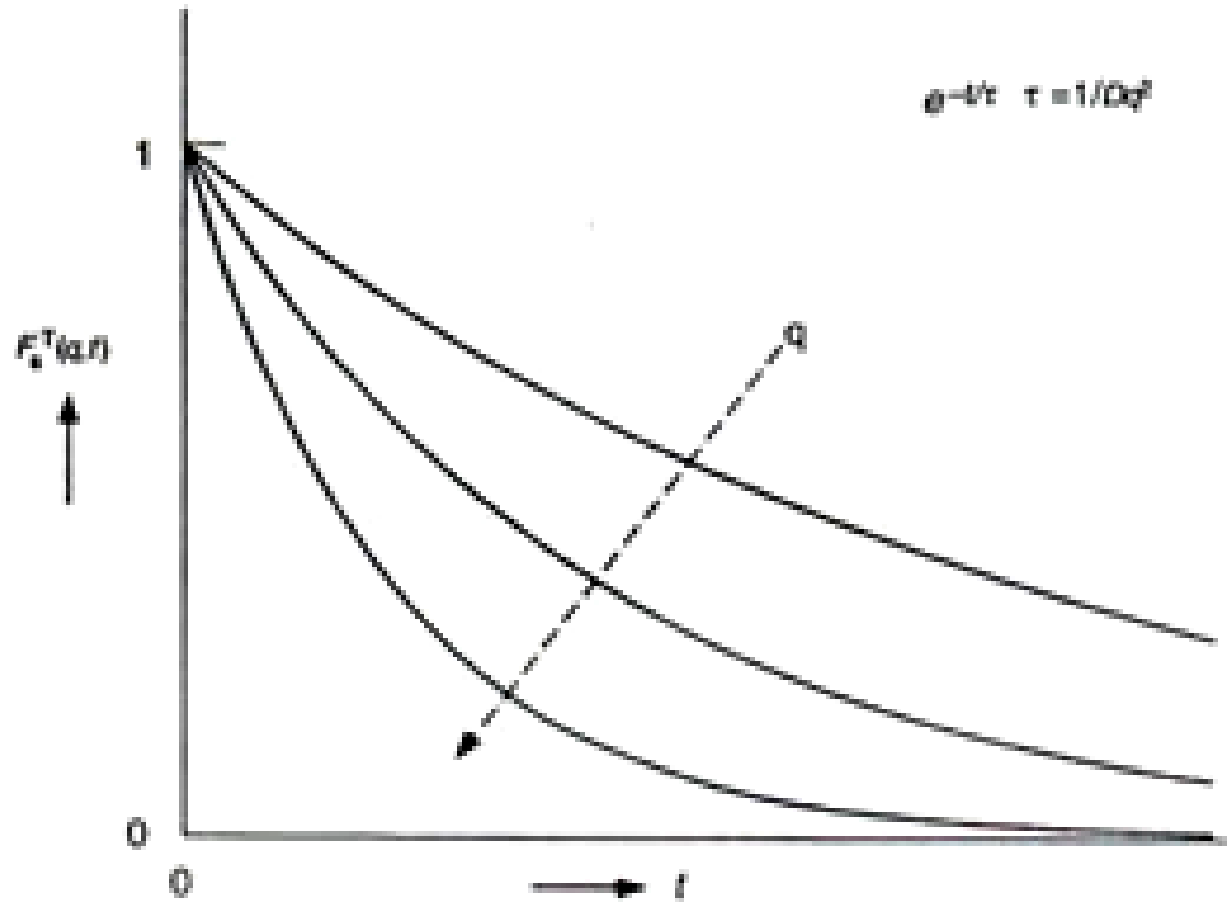

Figure 8.4 Plot of the incoherent intermediate scattering function $F_s^T(q, t)$ calculated for translational diffusion, for different q values.

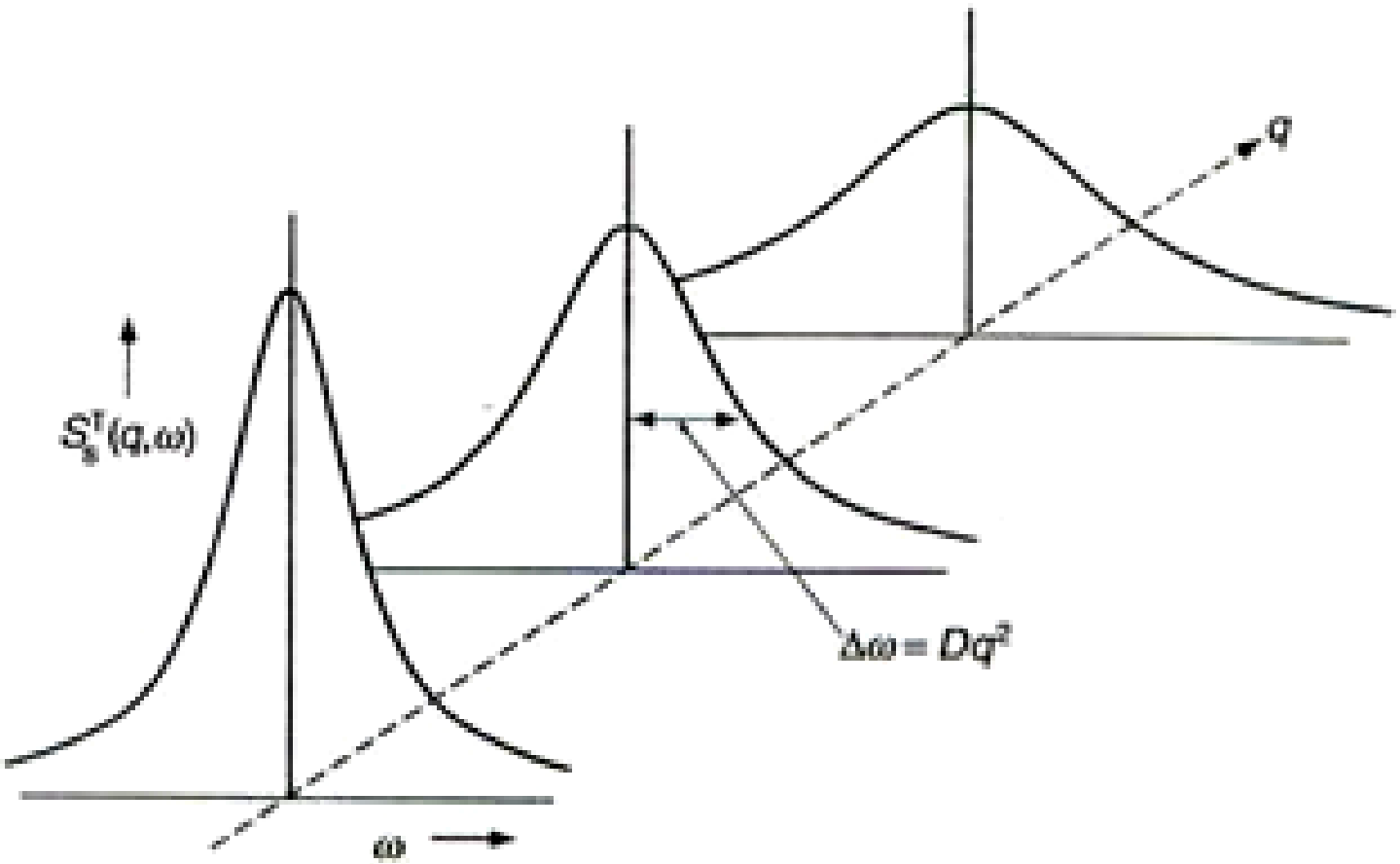

Figure 8.5 Schematic representation of the incoherent dynamic structure factor $S_s^T(q, \omega)$ for translational diffusion, at different q values.

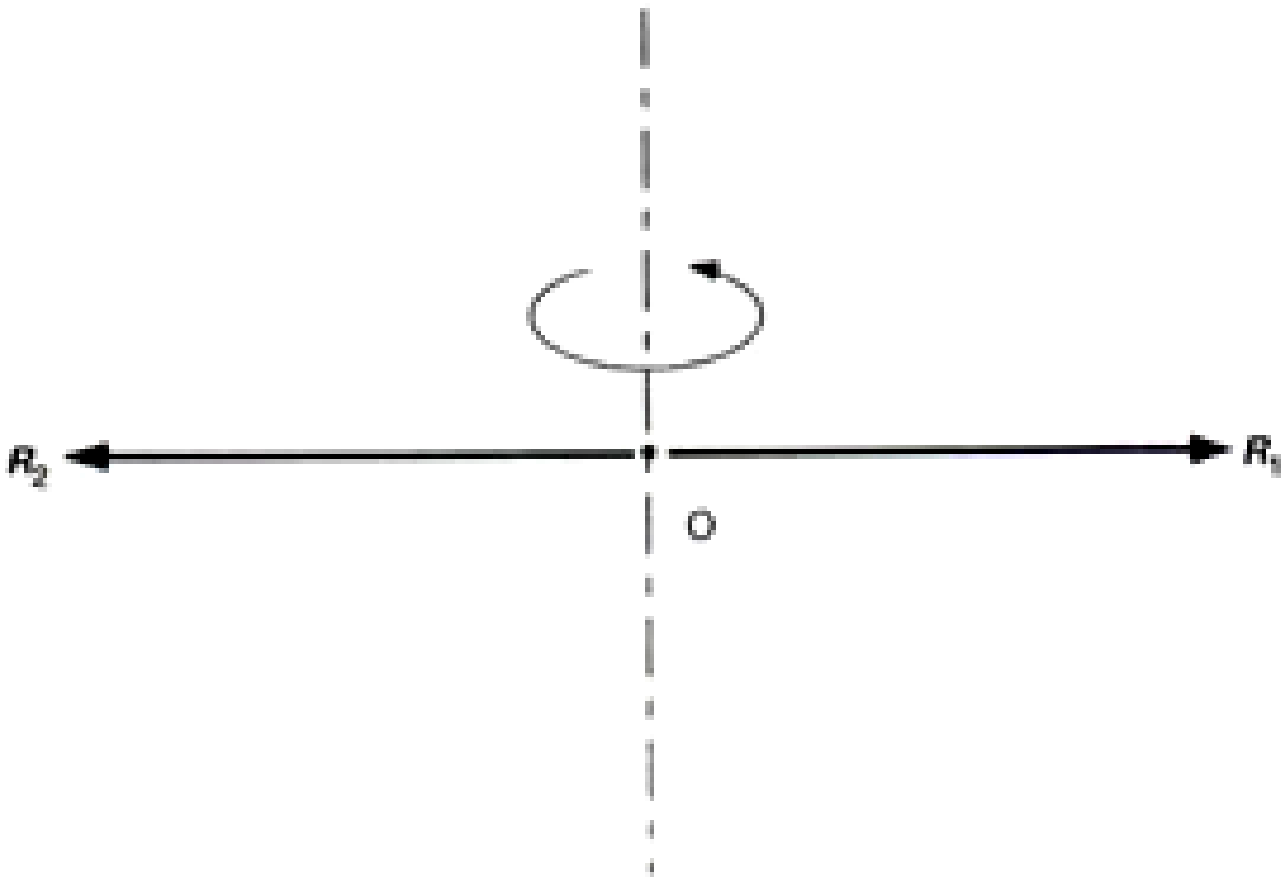

Figure 8.6 Schematics representing the simple model of rotational transitions between two sites R_1 and R_2.

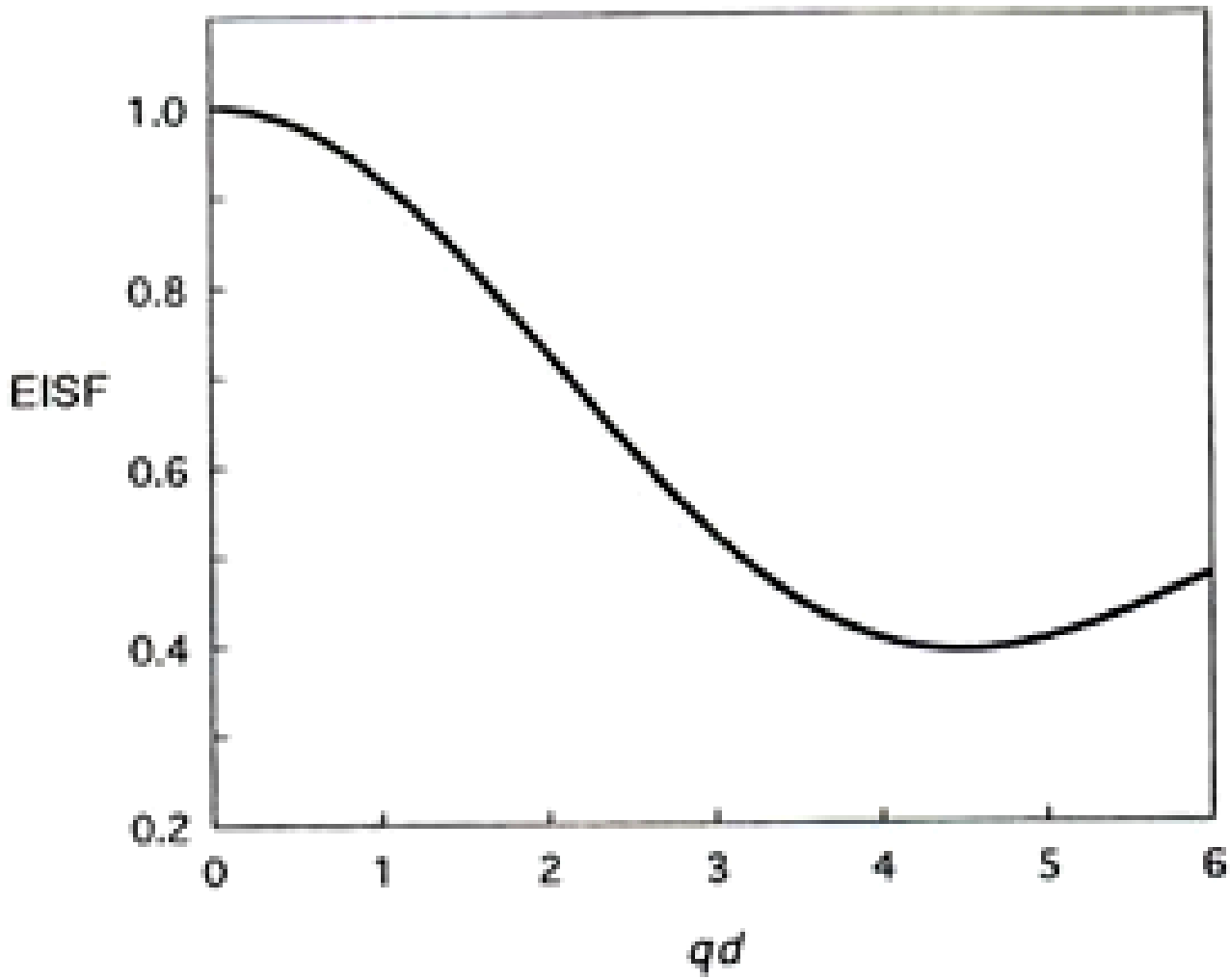

Figure 8.7 Elastic incoherent structure factor $A_0(q)$ calculated according to Equation (8.53) for the jump rotational motion between two sites.

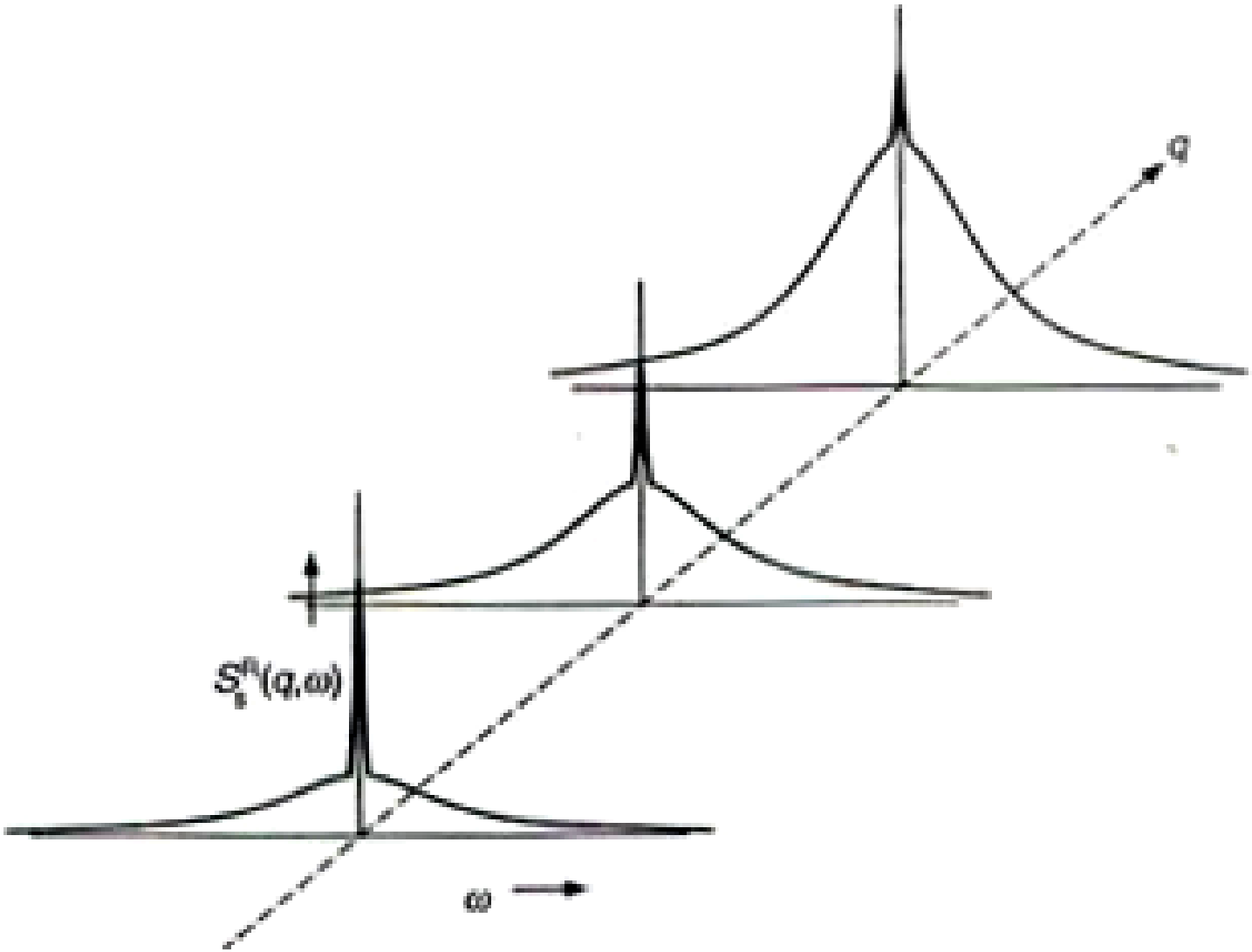

Figure 8.8 Schematic representation of the incoherent dynamic structure factor $S_s^R(q, \omega)$ for the rotational motion, at different q values.

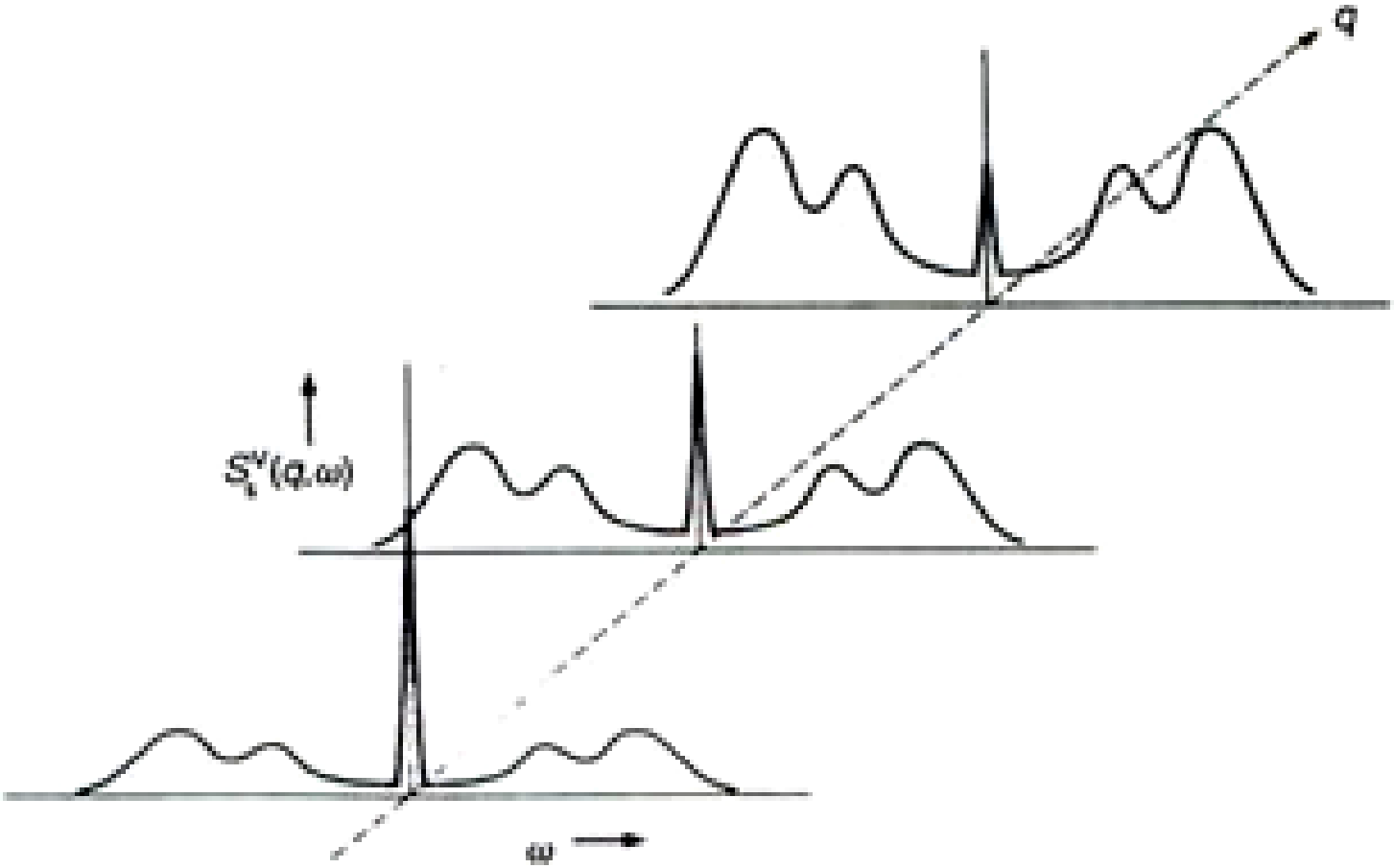

Figure 8.9 *Schematic representation of the incoherent dynamic structure factor* $S_s^V(q, \omega)$ *for vibration. at different* q *values.*

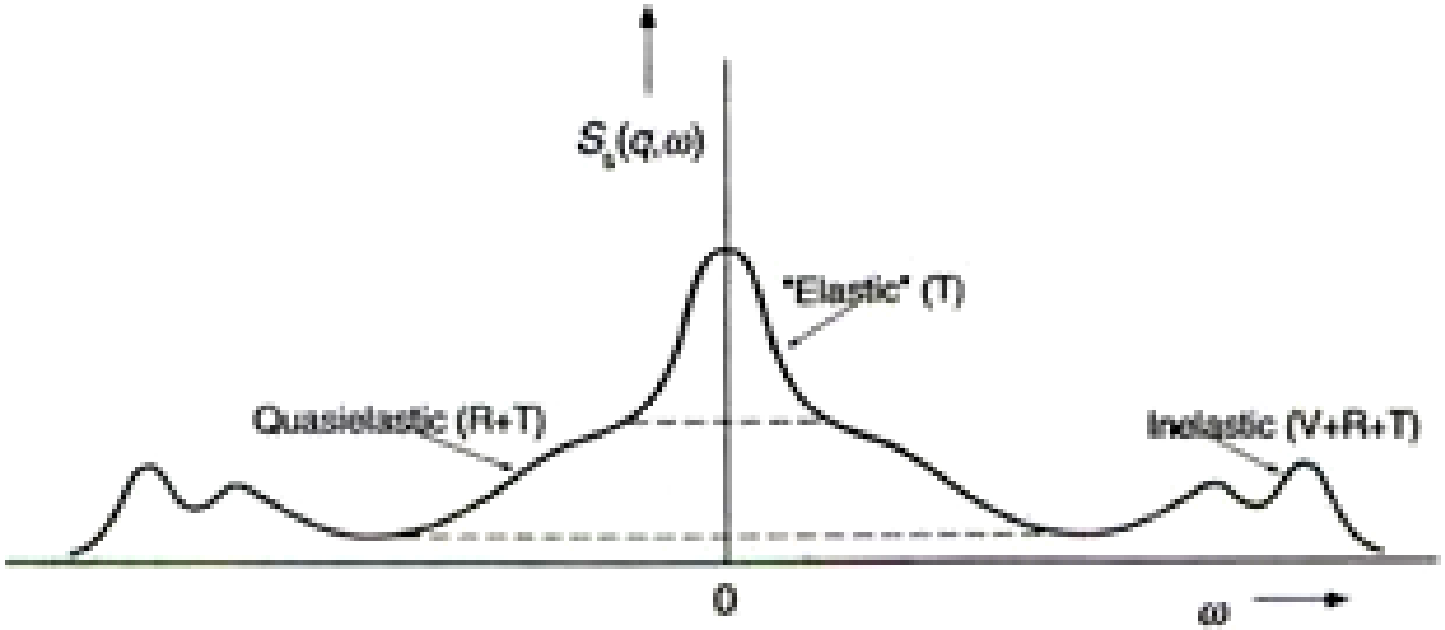

Figure 8.10 Schematic representation of the incoherent dynamic structure factor $S_s(q,\omega)$, at constant q, where translational (T), rotational (R), and vibrational (V) motions all make contributions.

Spectrometers

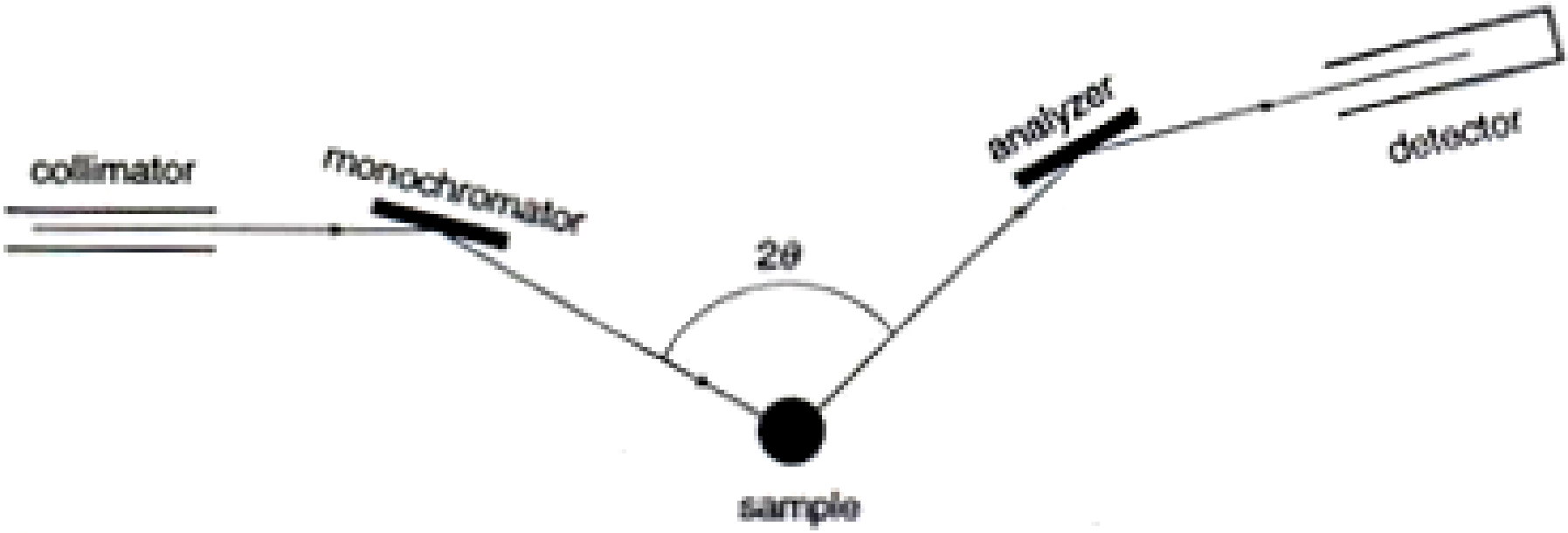

Figure 8.11 Schematic diagram of the triple-axis spectrometer. The three axes are at the monochromator crystal, the sample holder, and the analyzer crystal.

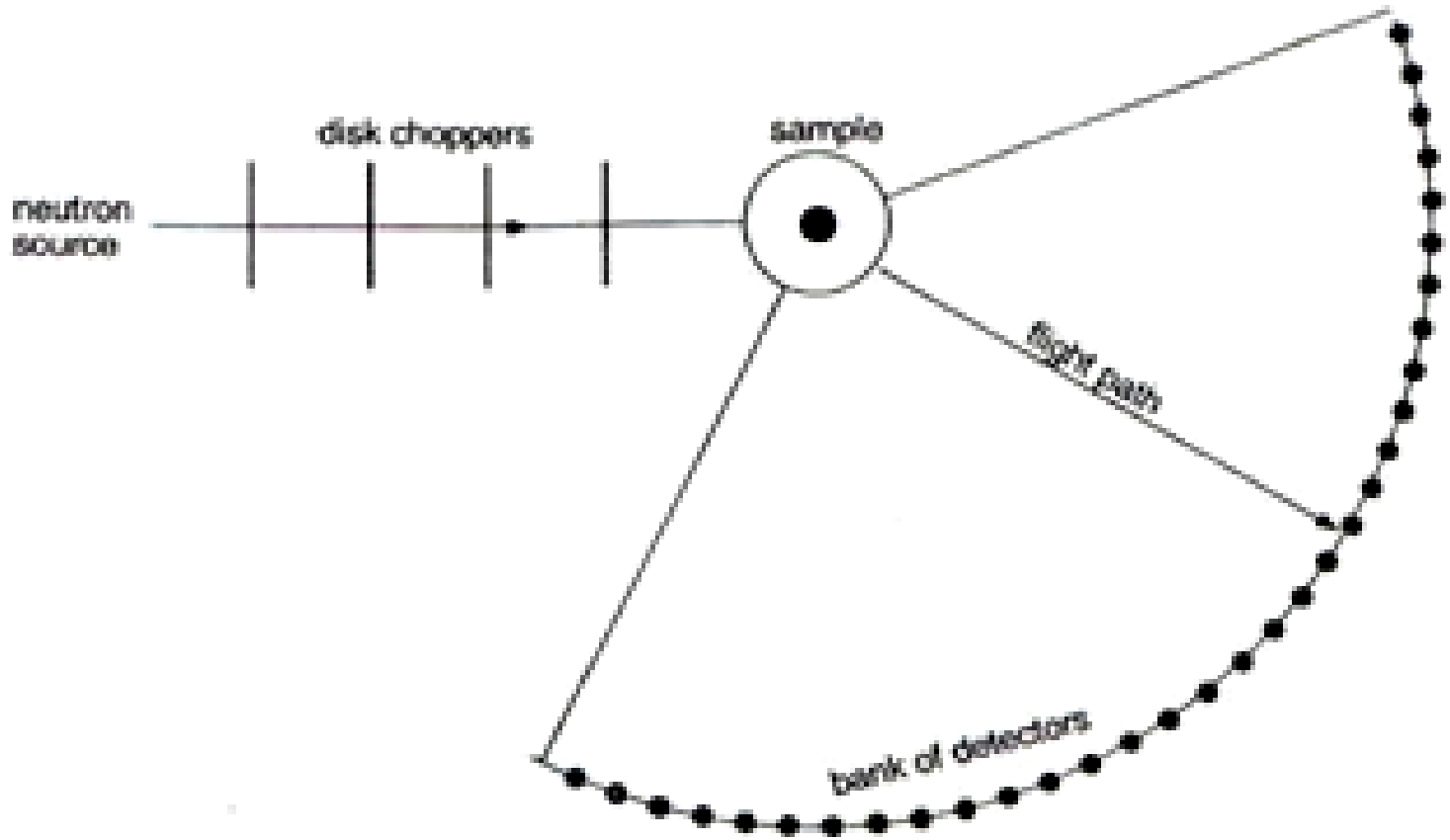

Figure 8.12 Schematic diagram of a time-of-flight spectrometer.

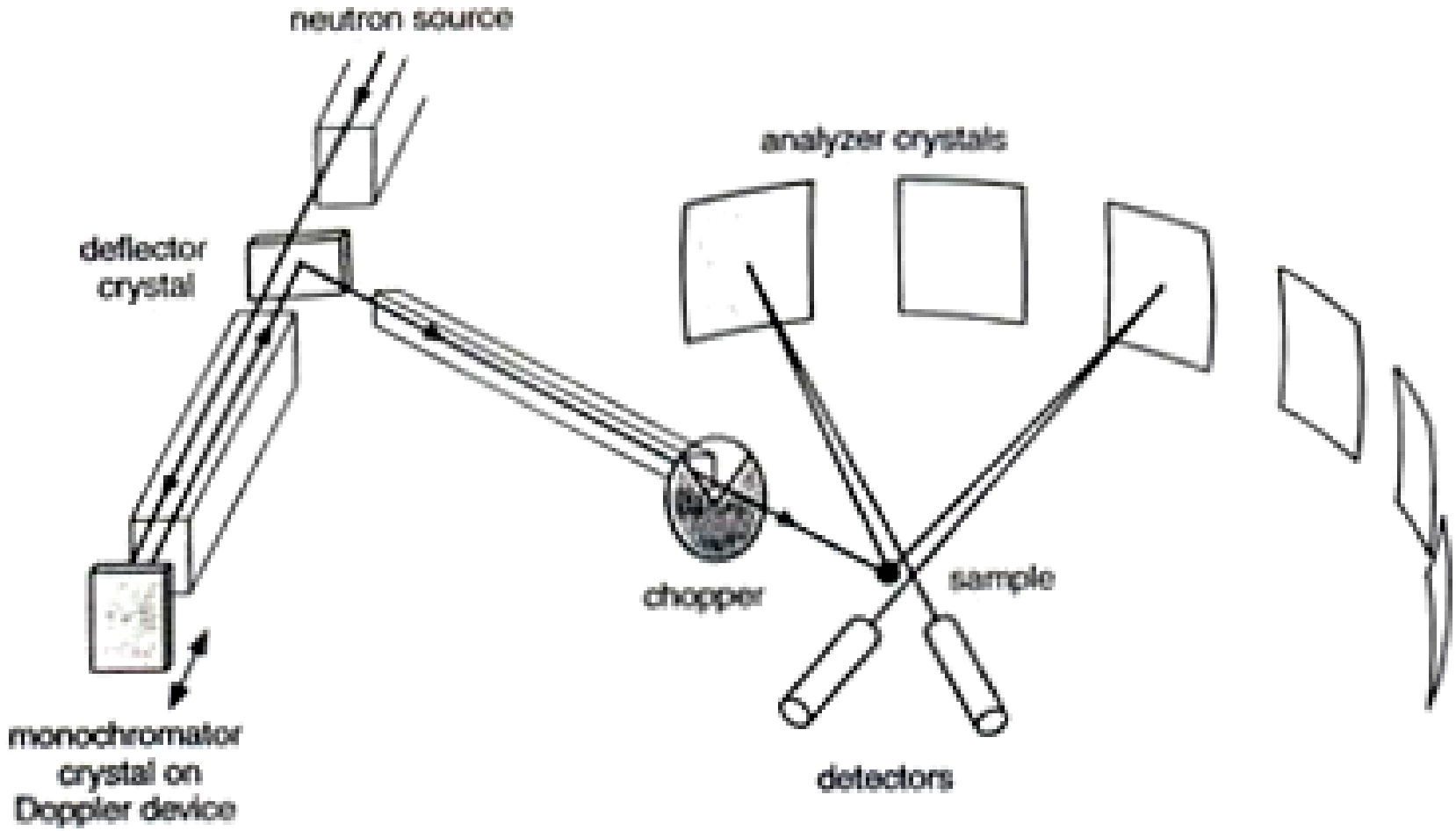

Figure 8.13 Schematic view of a back-scattering spectrometer. The neutrons incident from the neutron guide are back-scattered by the monochromator mounted on a Doppler drive, deflected by a graphite crystal to the sample, scattered to the analyzers and then back-scattered again to the detectors located close to the sample. The chopper interrupts the beam and makes it possible to discriminate the neutrons scattered directly into the detectors.

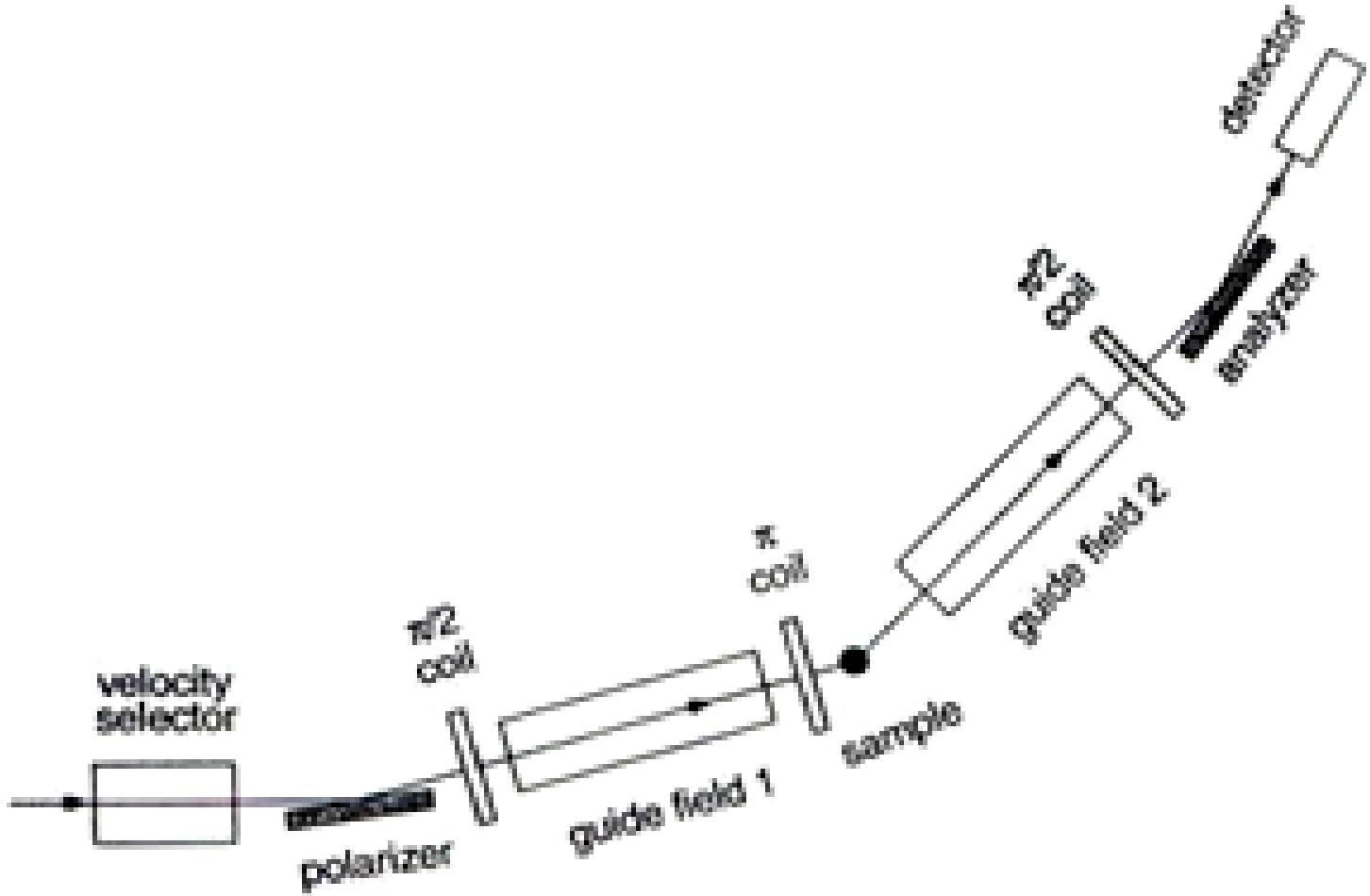

Figure 8.14 Schematic drawing of a neutron spin-echo spectrometer.

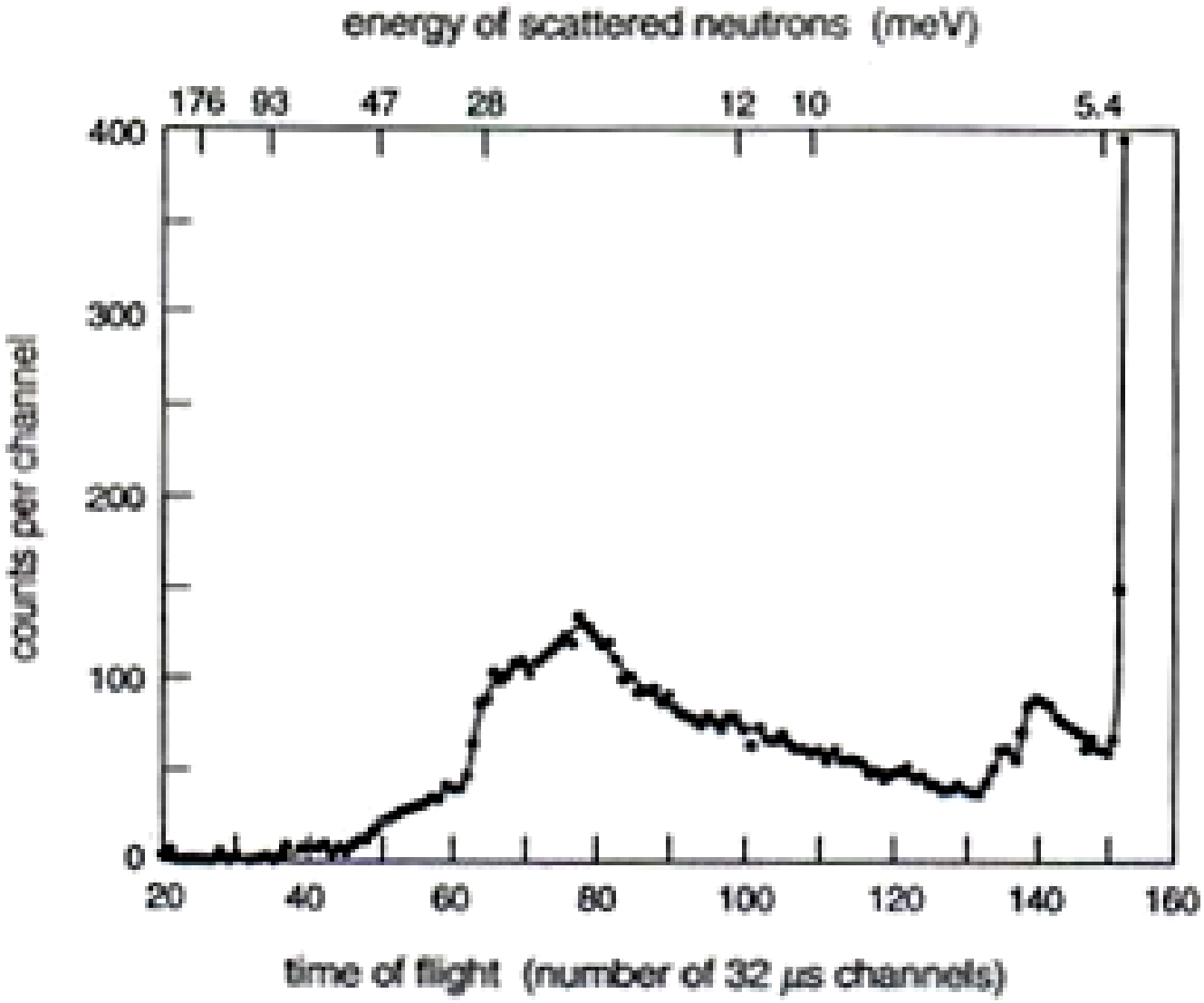

Figure 8.15 Time-of-flight spectrum obtained with linear polyethylene at 100 K. (From Danner *et al.*[11])

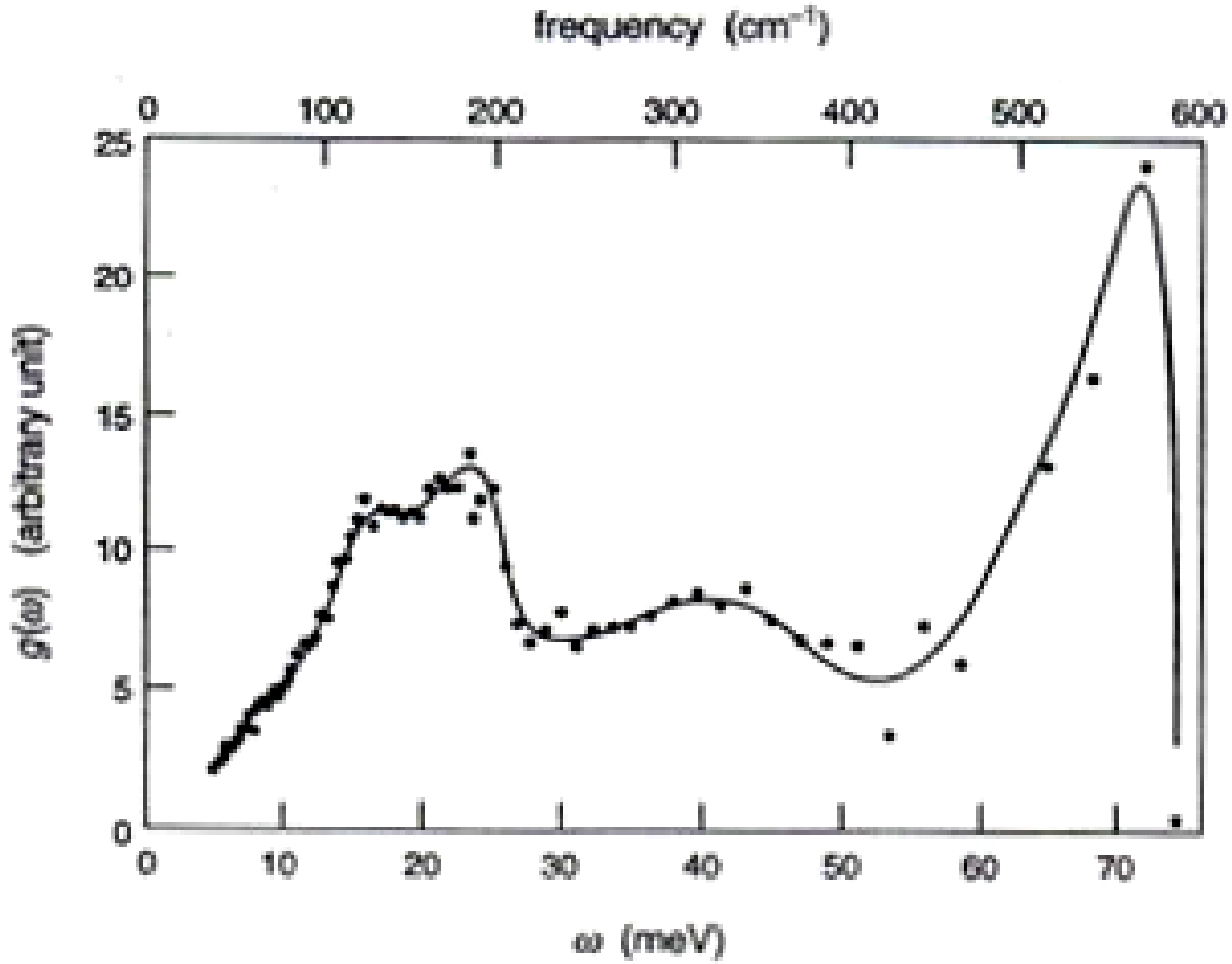

Figure 8.16 Density of vibrational states $g(\omega)$ of linear polyethylene derived, by use of Equation (8.66), from the time-of-flight spectrum shown in Figure 8.15. (From Danner *et al.*[11])

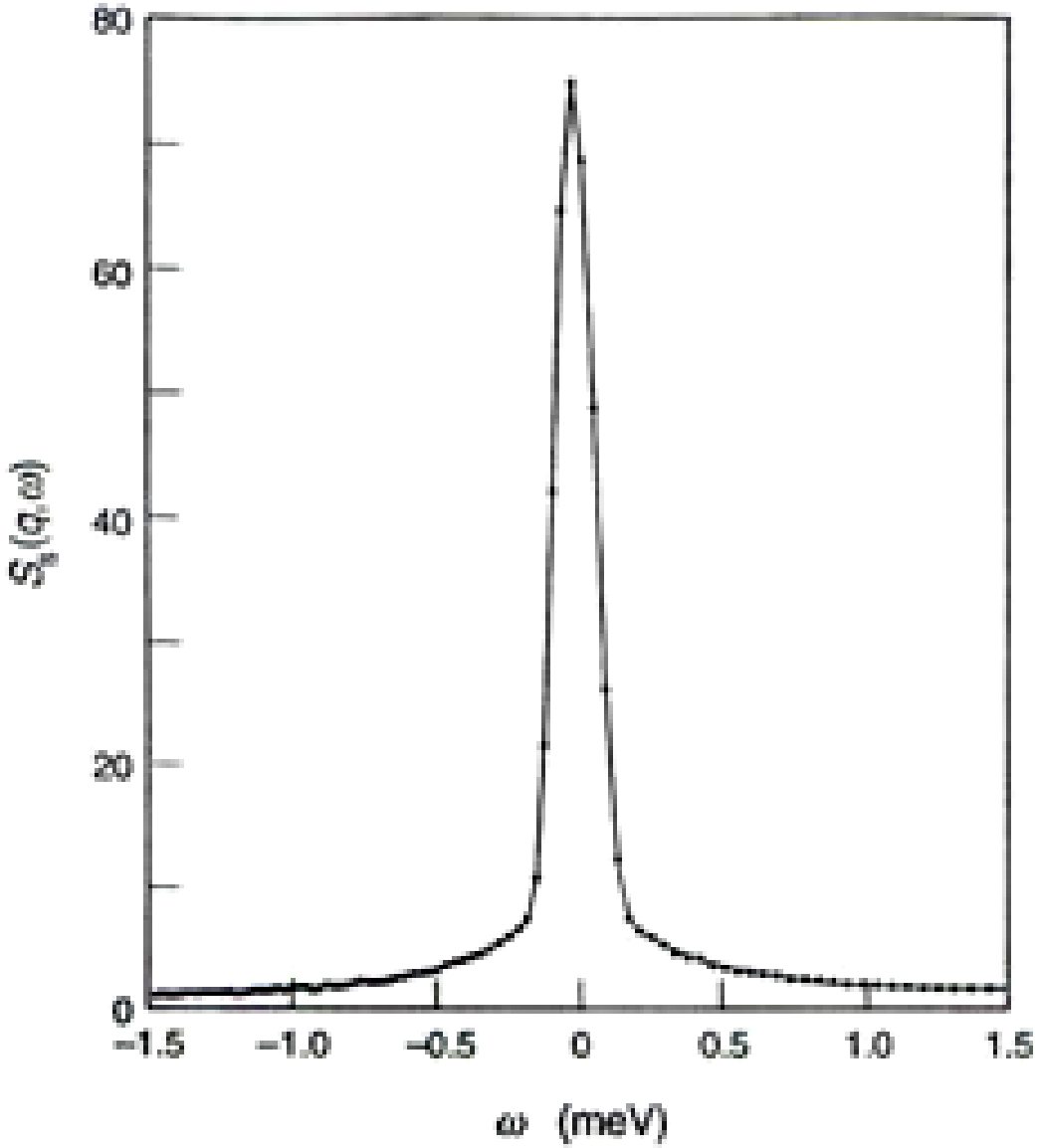

Figure 8.17 Dynamic structure factor $S_s(q, \omega)$ (predominantly incoherent) obtained, at 25°C, with a sample of poly(methyl methacrylate) in which all the hydrogens, except the ones in the ester methyl group, were replaced by deuteriums. (From Gabrys *et al.*[12])

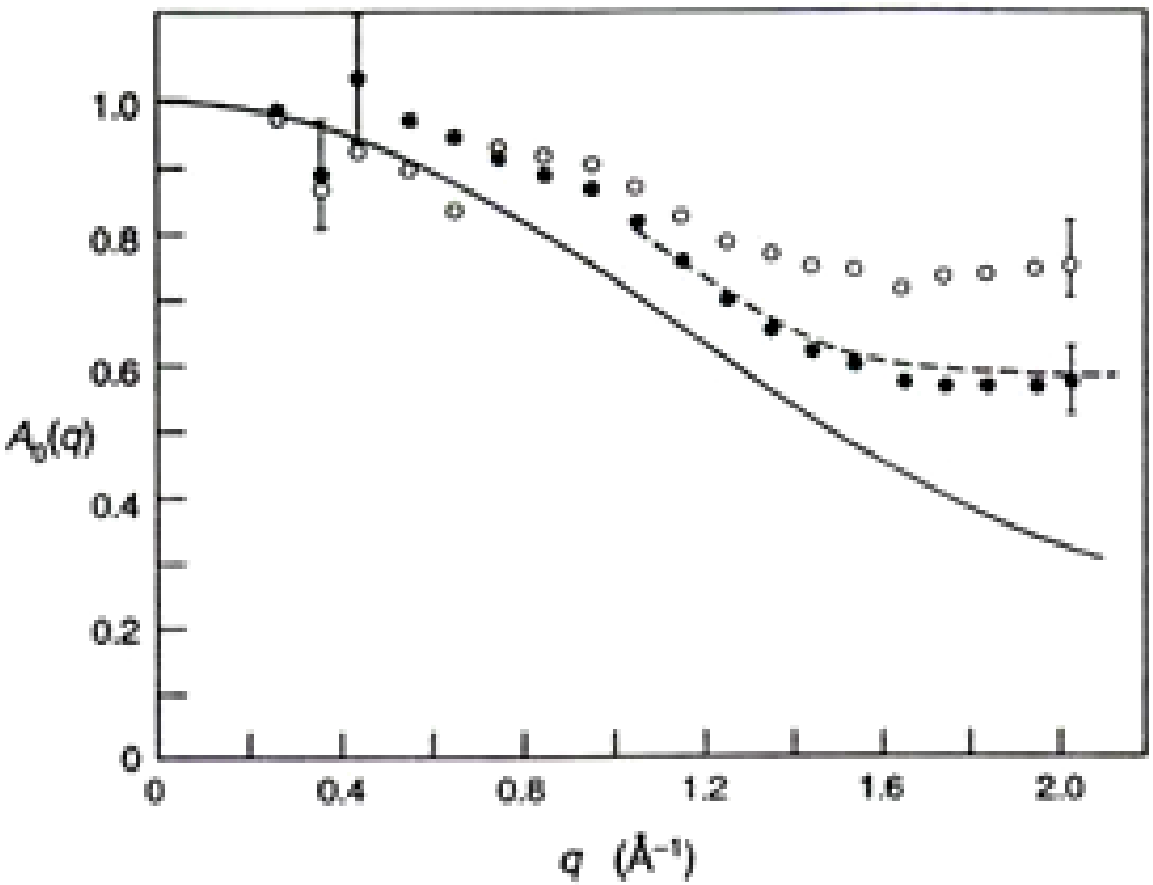

Figure 8.18 Elastic incoherent structure factor $A_0(q)$ obtained with poly(methyl methacrylate) at 150 K (open circles) and 290 K (solid circles). The theoretical prediction based on a model of rotation among three symmetric sites is given by the solid curve, whereas the broken curve was obtained by modifying the theoretical curve for the amount of contamination by coherent scattering in the experimental results. (From Gabrys *et al.*[12])

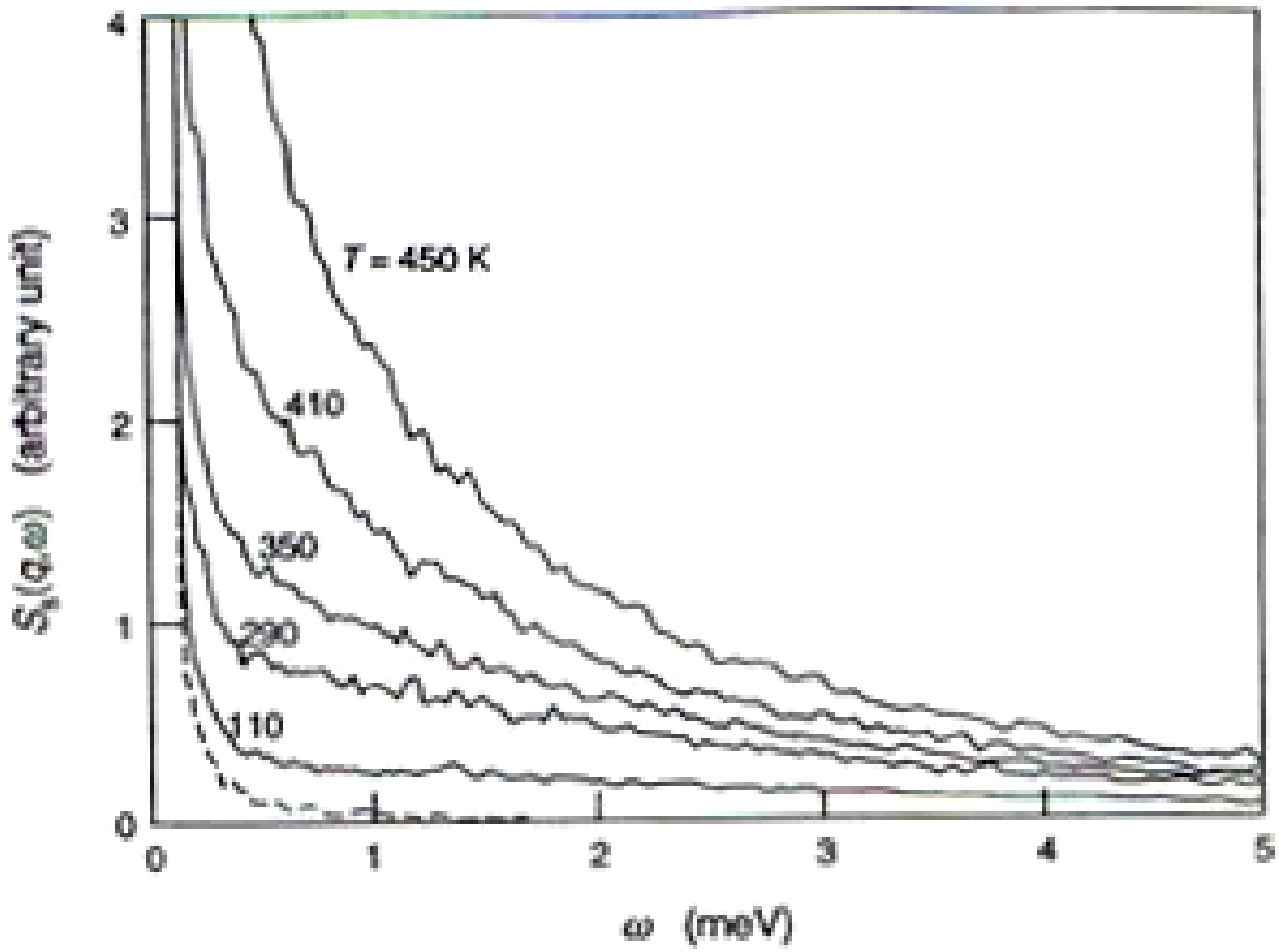

Figure 8.19 Incoherent dynamic structure factor measured with poly(vinyl chloride) for $q = 1.5\text{Å}^{-1}$ at temperatures above and below the glass transition temperature 358 K. The broken curve is the instrumental resolution function measured. (From Colmenero *et al.*[13])

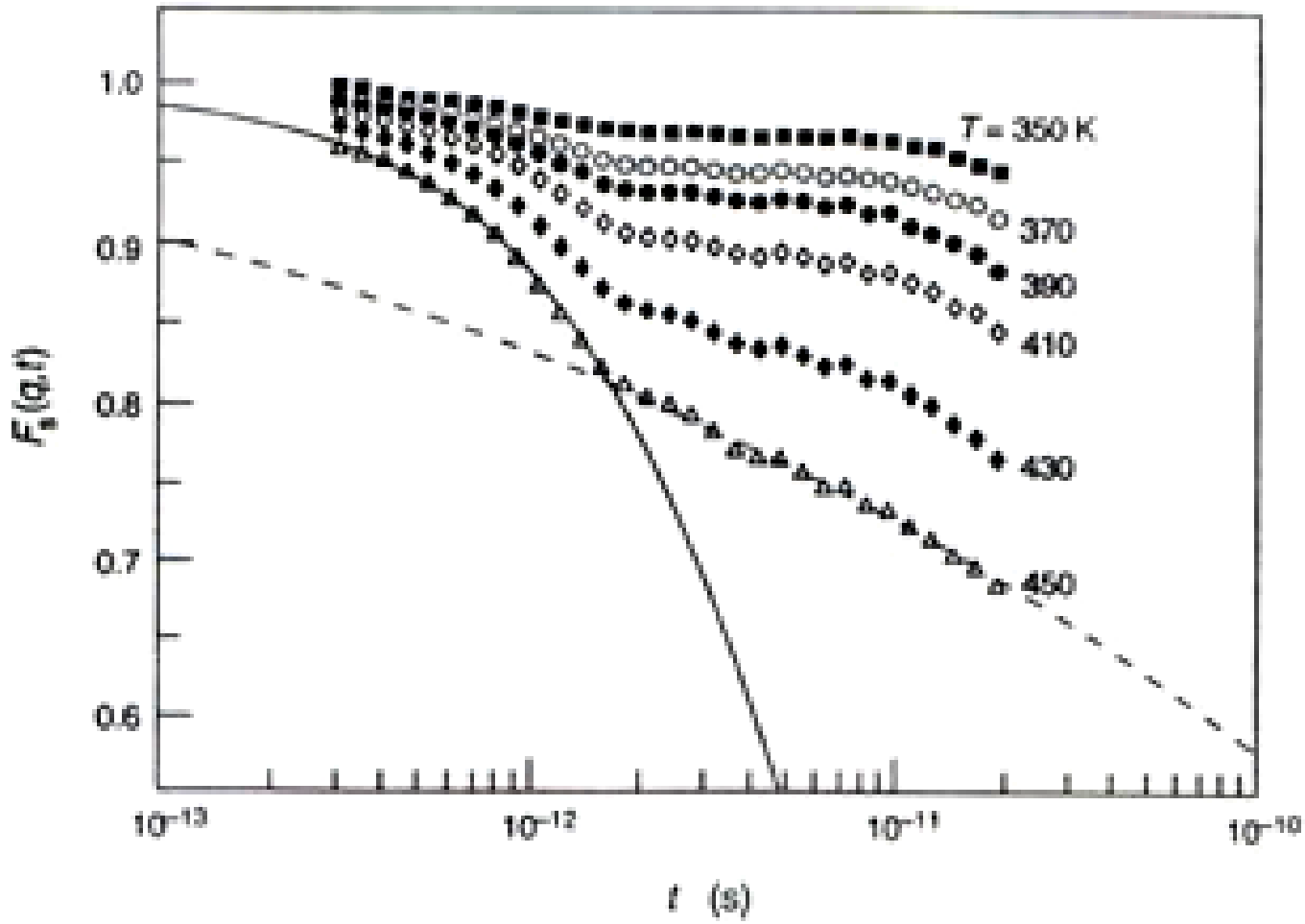

Figure 8.20 Intermediate scattering function obtained by Fourier transformation of $S_s(q, \omega)$ in Figure 8.19 from which the harmonic vibration contribution has been removed. (From Colmenero *et al.*[13])